

## Density Jump and Antenna Resistance in a High Pressure Helicon Plasma Source

Shinohara, Shunjiro

Department of Advanced Energy Engineering Science, Interdisciplinary Graduate School of Engineering Sciences, Kyushu University

Shamrai, Konstantin P.

Institute for Nuclear Research, 47 Prospekt Nauki, Kiev 28, 03680 MSP, Ukraine

<https://doi.org/10.15017/16583>

---

出版情報：九州大学大学院総合理工学報告. 22 (1), pp.23-27, 2000-06. 九州大学大学院総合理工学府  
バージョン：  
権利関係：

# Density Jump and Antenna Resistance in a High Pressure Helicon Plasma Source

Shunjiro SHINOHARA\* and Konstantin P. SHAMRAI\*\*

(Received February 17, 2000)

Antenna loading and density jump experimentally obtained by double  $m = 0$  antenna at high argon pressures of 51 and 6 mTorr are compared with the theory, which considers the conversion of helicon waves into electrostatic waves. The abrupt density jumps are found to depend strongly on the antenna spectrum. In a wide range of operation parameters, computed plasma load resistance, thresholds for density jumps and magnetic field profiles satisfactorily agree with experimental data.

## 1. Introduction

Helicon discharge<sup>1)2)</sup> attracts growing interest as a source of dense plasmas for various applications and basic research. Both experiments and theoretical models reported so far have been normally dealt with discharges at relatively low gas pressures ( $<10-20$  mTorr), when the electron collision frequency  $\nu_e$  is less or about  $\omega$ , the driving frequency. Helicon plasmas demonstrate abrupt jumps between low and high density modes. These jumps are identified with transitions between inductively coupled and wave coupled modes, and were measured in experiments with various devices<sup>3)-5)</sup> and interpreted theoretically<sup>6)-8)</sup>.

The area of high pressures, of order a few tens mTorr, is of interest for deposition technologies, where  $\nu_e$  is higher than  $\omega$ . Although a capability of high pressure helicon discharge was reported<sup>9)-11)</sup>, little experimental data are available in this area. In recent experiments<sup>12)</sup>, detailed measurements were performed on the discharge modes by double  $m = 0$  antenna and high Ar pressures, where the  $\nu_e/\omega$  ratio was about 10. It was found that jump-like transitions are intrinsic for the high pressure discharge as well as for the low pressure one.

In this paper, experimental data<sup>12)</sup> are compared in detail with computations on the basis of theoretical model<sup>6)</sup>, which takes into account, along with direct absorption of helicon waves due to collisions, the effect of mode conversion of helicons into electrostatic Trivelpiece-Gould (TG) waves.

## 2. Theoretical Model and Predictions

A theoretical model<sup>6)</sup> has been modified to perform computations for the conditions of experiments<sup>12)</sup>. A helicon source is considered as a uniform plasma column restricted in axial direction at  $z = R$  and  $L$  (see **Fig. 1**). Two loops of  $m = 0$  antenna are supposed to be of radius  $r_0$ , the same with the plasma column, and of finite width  $d$ . The density of azimuthal antenna current,  $j_a = i_a(z) \delta(r - r_0) \cos\omega t$  (and also electromagnetic fields  $\mathbf{E}$  and  $\mathbf{B}$ ), is represented as a sum of Fourier harmonics over axial discrete wavenumbers  $k = l_z\pi/\Delta z$  ( $\Delta z = R - L$  and  $l_z = 1, 2, \dots$ ). The spectral amplitudes  $i_k$  are shown in **Fig. 1** for the same and opposite directions of currents in the antenna loops.

Using Maxwell equations with dimensionless field amplitudes, one arrives at the following expression for the antenna load impedance,

\*Department of Advanced Energy Engineering Science

\*\*Institute for Nuclear Research, 47 Prospekt Nauki, Kiev 28, 03680 MSP, Ukraine

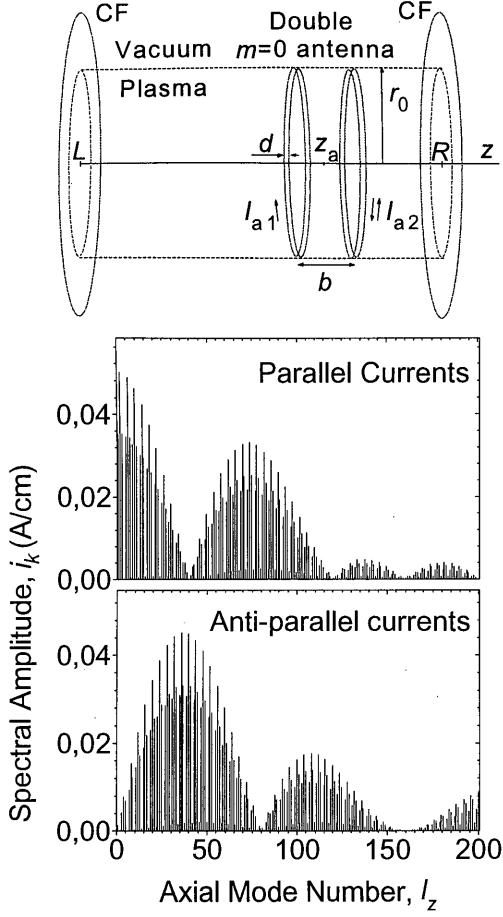


**Fig. 1** Theoretical model of helicon source (top), and computed antenna spectra for parallel and anti-parallel RF current directions (bottom). Conducting end-flanges are denoted as CF.

$$Z_a = - \frac{4\pi^2 r_0 \Delta z}{c} \sum \left| \frac{i_k}{I_a} \right|^2 e_{\theta k} (r = r_0), \quad (1)$$

where  $c$  is the speed of light, the sum is taken over all the harmonics,  $I_a$  is the amplitude of antenna current,  $e_{\theta k}$  is the complex amplitude of azimuthal electric field and CGS units are used. The plasma load impedance is defined as  $Z_p = Z_a - Z_v$  where  $Z_v$  is vacuum (without plasma) load impedance.

The permittivity tensor is considered in the following approximation,

$$\begin{aligned} K_1 &= 1 - (\omega_{pe}^2 \gamma_e / \Delta) - (\omega_{pi}^2 / \omega^2 \gamma_i) \\ K_2 &= \omega_{pe}^2 \omega_{ce} / \omega \Delta \end{aligned} \quad (2)$$

$$\begin{aligned} K_3 &= 1 + (k r_{De})^{-2} [1 - w(\xi)] \\ &\quad [1 - i(\nu_e / \omega \gamma_e) w(\xi)]^{-1}, \end{aligned}$$

where  $\omega_{pe, pi}$  ( $\omega_{ce}$ ) are the electron and ion plasma (electron cyclotron) frequencies,  $r_{De}$  is the electron Debye radius,  $\Delta = (\omega \gamma_e)^2 - \omega_{ce}^2$  and  $\gamma_{e, i} = 1 + i(\nu_{e, i} / \omega)$ .

Here,  $\nu_{e, i}$  are the electron and ion collision frequencies, and the effect of Landau damping (LD) is included in the component  $K_3$ .

$$\xi = \omega \gamma_e / 2^{1/2} k v_{Te}, \quad w(\xi) = \pi^{1/2} \xi \exp(-\xi^2) [\text{Erfi}(\xi) - i] \quad (3)$$

( $v_{Te}$ : electron thermal velocity,  $\text{Erfi}(\xi)$ : imaginary error function).

Considering the plasma-vacuum interface, analytic rf power was solved via two different mechanisms: direct absorption of helicon waves excited by antenna due to collisional and collisionless (Landau) damping<sup>13)</sup>, and a dominant absorption due to surface conversion of helicon waves into TG waves<sup>6)</sup>. Although TG waves are strongly damped at high collisions, the efficiency of this conversion mechanism turns out to be very high at  $\nu_e > \omega$ , as well as at  $\nu_e < \omega$ .

Obtained expressions for fields and plasma load resistance were computed using numerical values as follows (see **Fig. 1** and ref. 12):  $L = -80$  cm,  $R = 0$  cm,  $r_0 = 2.5$  cm,  $z_a = -20$  cm,  $b = 2$  cm,  $d = 1$  cm, and  $|I_{a1}| = |I_{a2}| = 1$  A. **Fig. 2** shows the variation with density of real (resistance) and imaginary (reactance) parts of the plasma load impedance with the use of the relation (1). Note that  $R_p = R_a$ , as long as vacuum load resistance is neglected in theory. One can see from **Fig. 2** that plasma resistance is low sensitive to the electron temperature, and thus to the electron collision frequency, as well as to the effect of Landau damping.

In a low collision case, the variation of resistance with density and/or magnetic field is substantially non-monotonic<sup>8)</sup>. It demonstrates a set of maxima and minima due to the contribution in absorption of various axial and radial modes. At high collisions, the variation

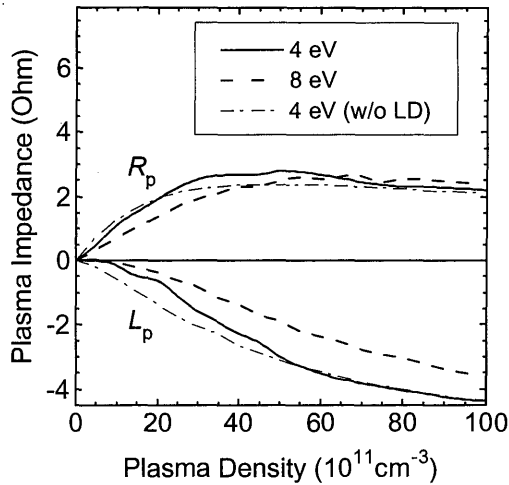


**Fig. 2** Computed variation with density of plasma load resistance ( $R_p$ ) and reactance ( $L_p$ ), for parallel antenna currents. Magnetic field  $B_0 = 100$  G and Ar pressure  $p_{Ar} = 51$  mTorr.

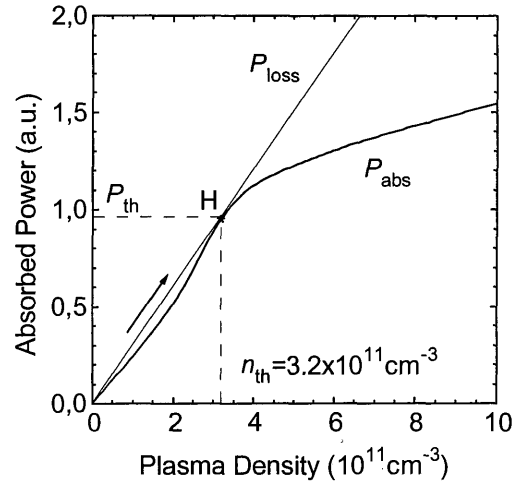
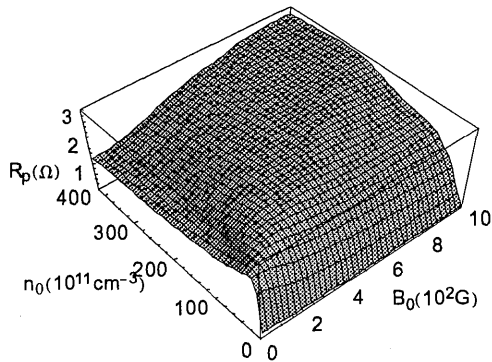


**Fig. 4** Absorption curve at critical parallel antenna currents corresponding to coupling of the discharge to the high mode of density  $n_{th}$  ( $p_{Ar} = 6$  mTorr and  $T_e = 8$  eV). The jump to the point H, shown by arrow, occurs at a critical absorbed power  $P_{th}$ . A straight line shows the plasma loss  $P_{loss} = \alpha n_0$ .

**Parallel Currents**



**Anti-parallel currents**

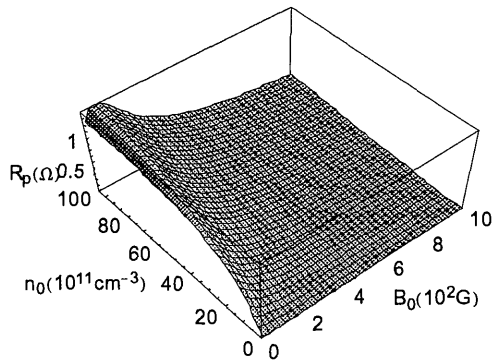


**Fig. 3** Computed dependences of plasma resistance on density and magnetic field, for parallel and anti-parallel antenna currents:  $p_{Ar} = 5$  mTorr and  $T_e = 4$  eV.

of resistance is found to be quite smooth: see **Fig. 3** at  $p_{Ar} = 51$  mTorr. From this figure (anti-parallel currents), the resistance makes substantial values at low magnetic fields, and drops rapidly with increasing  $B_0$ . The reason is that antenna excites only short helicon waves (see **Fig. 1** where the first spectral maximum for anti-parallel currents is around  $l_z \approx 35$ ), and the threshold on density for the excitation of helicons can be understood from ref. 6.

In papers<sup>(6)(8)</sup>, a jump of the helicon discharge to the high density mode was interpreted using the following power balance arguments. With growing antenna current, the absorption curve,  $P_{abs}$  as a function of density  $n_0$ , increases in amplitude. When the antenna current reaches some critical value, this curve touches the loss line,  $P_{loss} = \alpha n_0$  ( $\alpha$ : some coefficient). Then the density jump occurs, as shown in **Fig. 4**, from zero plasma density to  $n_0 = n_{th}$ .

**3. Comparison of experimental and theoretical results**

Experiments have been performed with a 5 cm in diameter source attached to a 170 cm long drift chamber<sup>(3)(12)(14)</sup>. The discharge was excited at frequency  $\omega/2\pi = 7$  MHz by double  $m = 0$  antenna, both at the same and opposite directions of RF currents. Data were taken in a wide

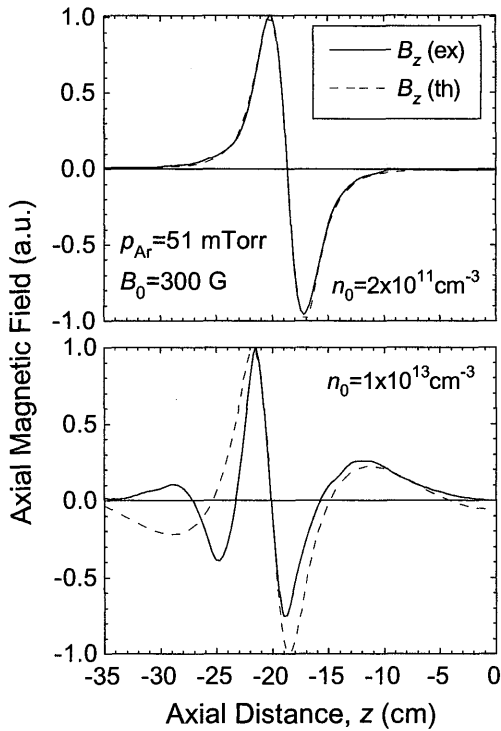


**Fig. 5** Comparison of experimental and theoretical axial profiles of the  $B_z$  ( $r = 0$ ) magnetic field excited with anti-parallel currents. The top and bottom figures correspond to the low density (before the jump) and high density (after the jump) modes, at  $B_0 = 300$  G and  $p_{Ar} = 51$  mTorr.

antenna loading resistance, which also demonstrates jumps, and of axial and radial profiles and phases of the magnetic field, and results are compared here with computations.

**Fig. 5** shows experimental and computed axial profiles of the  $B_z$ , before and after the density jump. One can see that in low density mode antenna excites evanescent field. The agreement of theory with experiment is pretty good. In the high density mode theory predicts a deeper penetration of field (wave coupling) into downstream plasma than the experiment.

Comparison of measured and computed load resistances was executed for different conditions, changing pressure, magnetic field and antenna current directions, and fairly good agreements were found. **Fig. 6** shows an example of the computed and measured resistances as a function of plasma density. Threshold densities for jump are very close in theory and experiment, but the agreement does not improve at high densities because measured radial nonuniformity is higher in this case.

We have also compared experimental and theoretical dependences of plasma resistance on input power. The agreement of theory and experiment on the plasma resistance versus normalized power is good within 50% for various conditions. Here, for convenience, we use the values of input power, for experiment, and absorbed power, for theory, both normalized by threshold powers for the density jump,  $P_{th}$ .

Predictions of density jumps were based on an assumption that plasma losses in the discharge scale linearly with density,  $P_{loss} = \alpha n_0$ . To verify if it is so in our experiments, we have plotted in **Fig. 7** a number of experimental points for the discharge at  $p_{At} = 51$  mTorr in various conditions. As seen, the variation of density with input power is nearly linear in the high density mode ( $n_0 > n_{th}$ ,  $P_{in} > P_{th}$ ). This means that losses are also linear with density, because of the balance condition,  $P_{in} = P_{loss}$ .

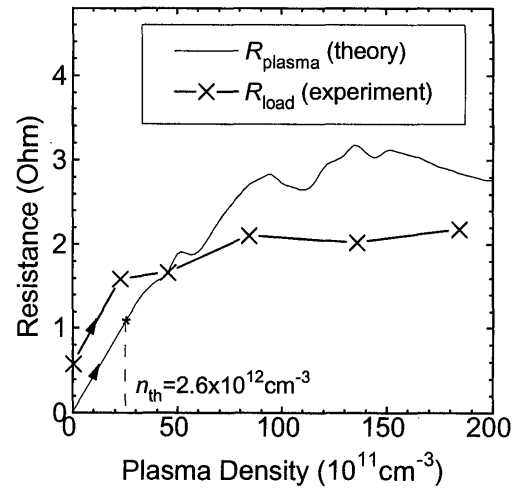


**Fig. 6** Comparison of experimental and theoretical dependences on density of the plasma load resistance for parallel antenna currents at  $p_{Ar} = 51$  mTorr and  $B_0 = 300$  G. Experimental threshold density  $n_{th} = 2.4 \times 10^{12}$   $\text{cm}^{-3}$ .

range of magnetic fields, 0 to 1000 G, and input powers, up to 2500 W. The high density mode in the range of  $10^{13}$   $\text{cm}^{-3}$  could be attained at input powers of 100 to 1000 W, depending on the magnetic field, relative directions of RF currents and gas pressure.

Detailed measurements were conducted of the

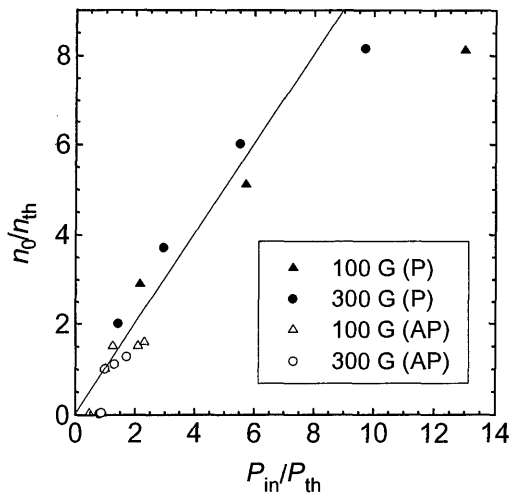


**Fig. 7** Experimental data on normalized plasma density vs input power, for various discharge modes. Solid line corresponds to  $n_0/n_{th} = P_{in}/P_{th}$ . P and AP refer to the parallel and anti-parallel current directions.

#### 4. Conclusion

A quite simple model, which takes into account the mode conversion of helicon waves into TG waves, is compared with the experimental results on antenna loading, density jump and the profiles of magnetic field obtained by double  $m = 0$  antenna at high argon pressures of 51 and 6 mTorr. Theory can explain, within a factor of 1.5, dependences of plasma load resistance on plasma density and input power. Using the power balance arguments permits one to interpret abrupt density jumps in discharge, and predicts jump thresholds, both on density and input power, to increase with the increase of magnetic field and gas pressure, and with shortening the wavelengths excited by antenna.

#### Acknowledgements

One of the authors (KPS) is grateful for a hospitality to members of the laboratory of Prof. Y. Kawai. His continuous encouragement of this work is appreciated. KPS acknowledges with thanks a support of his visit to Kyushu University by the Venture Business Laboratory.

#### References

- 1) R. W. Boswell and F. F. Chen, IEEE Trans. Plasma Sci., **25**, 1229 (1997).
- 2) S. Shinohara, Jpn. J. Appl. Phys., **36**, 4695 (1997).
- 3) S. Shinohara, Y. Miyauchi and Y. Kawai, Plasma Phys. Control. Fusion, **37**, 1015 (1995).
- 4) A. R. Ellingboe and R. W. Boswell, Phys Plasmas, **3**, 2797 (1996).
- 5) D. D. Blackwell and F. F. Chen, Plasma Sources Sci. Technol., **6**, 569 (1997).
- 6) K. P. Shamrai, V. P. Pavlenko and V. B. Taranov, Plasma Phys. Control. Fusion, **39**, 505 (1997).
- 7) Y. Mouzouris and J. E. Scharer, Phys Plasmas, **5**, 4253 (1998).
- 8) K. P. Shamrai, Plasma Sources Sci. Technol., **7**, 499 (1998).
- 9) F. F. Chen, J. Vac. Sci. Technol., A **10**, 1389 (1992).
- 10) T. Mieno, T. Shoji and K. Kadota, Jpn. J. Appl. Phys., **31**, 1879 (1992).
- 11) G. R. Tynan, A. D. Bailey, G. A. Campbell, R. Charatan, A. de Chambrier, G. Gibson, D. J. Hemker, K. Jones, A. Kuthi, C. Lee, T. Shoji and M. Wilcoxson, J. Vac. Sci. Technol., A **15**, 2885 (1997).
- 12) S. Shinohara and K. Yonekura, Plasma Phys. Control. Fusion, **42**, 41 (2000).
- 13) F. F. Chen, Plasma Phys. Control. Fusion, **33**, 339 (1991).
- 14) S. Shinohara, N. Kaneda and Y. Kawai, Thin Solid Films, **316**, 139 (1998).